

Macromolecular Research

Volume 16, Number 3 April 30, 2008

© Copyright 2008 by the Polymer Society of Korea

Communications

Annealing Temperature Effect of Hole-Collecting Polymeric Nanolayer in Polymer Solar Cells

Youngkyoo Kim*, Minjung Shin, and Hwajeong Kim

Organic Nanoelectronics Laboratory, Department of Chemical Engineering, Kyungpook National University, Daegu 702-701, Korea

Received January 8, 2008; Revised February 16, 2008

Introduction

Recent pronounced global warming has attracted keen interest in solar cells due to their renewable feature exploiting tremendous solar energy (89 PW) during sun's lifetime of ~5 billion years.¹ Of the solar cells invented so far, inorganic solar cells are now in market but they have a demerit such as high fabrication cost and hard characteristics of inorganic materials which restrict the spreading of solar cells.² In this regard organic solar cells have been studied as a contingency because of their potential for cheaper manufacturing cost and variety of applications owing to flexible and semitransparent features.^{3,4}

To date, the most widely used polymer as a light-absorbing material is regioregular poly(3-hexylthiophene) (P3HT) which does also act as an electron-donating (i.e., hole-accepting) component in a bulk heterojunction layer inside corresponding solar cell geometry.⁵⁻⁸ Here we note that the bulk heterojunction film is, broadly speaking, a mixture of electron-donating and electron-accepting materials, whilst in more specific terms it has integrated and randomly

distributed p-n junctions in the bulk polymeric film.² As an electron-accepting material, soluble fullerenes such as 1-(3-methoxycarbonyl)-propyl-1-phenyl-(6,6)C₆₁ (PCBM) are widely used.

Considering the principle of electron flows in the bulk heterojunction polymer solar cells, it is not necessary to insert a low work function metal in between the bulk heterojunction layer and the electron-collecting electrode, which has been proven in our previous report.⁵ However, the direct hole collection from the bulk heterojunction layer to transparent conducting oxide, mostly indium tin-oxide (ITO), was not efficient owing to the insufficient interfacial contact between the bulk heterojunction layer and the ITO surface.² Hence most of efficient organic solar cells employ a buffer layer, in most cases poly(3,4-ethylenedioxythiophene): poly(styrenesulfonate) (PEDOT:PSS), between the bulk heterojunction layer and the ITO layer.^{2,4,9}

However, the influence of thickness and thermal annealing conditions of PEDOT:PSS layer was not much studied. In this work, we have briefly investigated the effect of thermal annealing temperature on the performance of polymer solar cells with the PEDOT:PSS nanolayer of which thickness is 20 nm. The result showed that about 40% power conversion efficiency was improved by thermal annealing of the PEDOT:PSS layer at 120 °C.

Results and Discussion

The blend solution of P3HT and PCBM (P3HT:PCBM =1:1 by weight) was prepared using chlorobenzene as a solvent at a solid concentration of 30 mg/mL. This solution was vigorously stirred for more than 2 days to dissolve all of solid particles in the solvent. Prior to making the polymer solar cells, the solution of PEDOT:PSS (Baytron AI 4083) was subjected to sonication for 15 min and then filtered using a Teflon membrane filter (pore size = 0.45 μm). On top of the precleaned ITO-coated glass, the filtered PEDOT:PSS solution was poured and then spin-coated to make 20 nm thick film. Next, the PEDOT:PSS coated substrate was thermally annealed for 15 min at 25, 120, and 200 °C.

*Corresponding Authors. E-mail: ykimm@knu.ac.kr

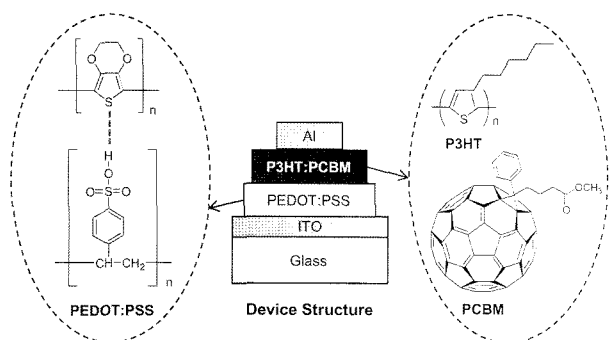


Figure 1. Device structure of polymer solar cells fabricated in this study and chemical structure of corresponding materials used for each layer.

On top of the three samples the P3HT:PCBM films were spin-coated for 30 sec at 2,500 rpm, which resulted in the 90 nm active layer. These samples were put into a vacuum chamber and then aluminum top electrode (80 nm thick) was deposited on the P3HT:PCBM layer. The structures of materials and devices are shown in Figure 1. We note that the P3HT:PCBM layer was not annealed in order to investigate the intrinsic influence of PEDOT:PSS layer upon thermal annealing, since the bestowing PEDOT:PSS layer under the active layer could be changed if the devices are thermally annealed at the well-known optimum temperature ($\sim 140^\circ\text{C}$).^{5,8}

The performance of the fabricated devices was measured in a nitrogen atmosphere. The current density-voltage (*J-V*) characteristics were measured using a solar cell measurement system equipped with an electrometer (Keithley 2400) and a solar simulator (Oriol). The incident light intensity was 85 mW/cm^2 at air mass (AM) 1.5 condition. The external quantum efficiency (EQE) of the devices was measured using a home-built system equipped with a Xe light source,

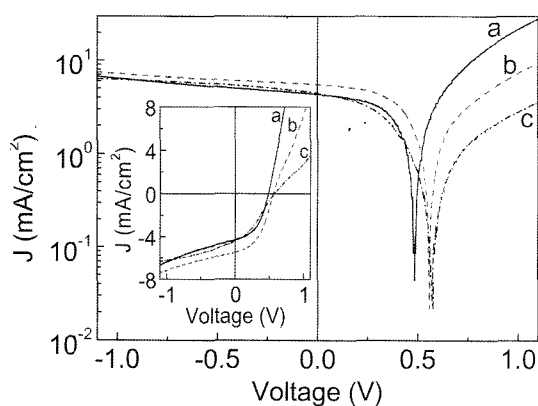


Figure 2. Light (AM 1.5, 85 mW/cm^2) *J-V* characteristics of polymer solar cells with the PEDOT:PSS layer annealed at 25°C (a: black solid line), 120°C (b: red dashed line), and 200°C (c: blue dash-dot line): Inset shows the same *J-V* curves in a linear scale.

a monochromator (CVI 110), and an electrometer (Keithley 2400). The incident light intensity was 6.15 mW/cm^2 at 480 nm.

As shown in Figure 2, the short circuit current density (J_{SC}) was markedly increased by annealing the PEDOT:PSS layer at 120°C (compared to the annealing at 25°C). This indicates that at around short circuit condition the charge transport (hole collection) through the PEDOT:PSS layer was improved by annealing at 120°C because the electron collection condition was same for all devices. The larger photocurrent for the device with the PEDOT:PSS layer annealed at 120°C was maintained for whole voltage ranges below the open circuit voltage. However, the *J-V* curve shape at above the open circuit voltage reflects that the series resistance became bigger for the device with the PEDOT:PSS layer annealed at 120°C than that annealed at 25°C . This trend is also proven from the dark *J-V* characteristics in Figure 2.

Here we need to discuss about the direction of hole transport. Below the open circuit condition (voltage) the hole charges flow from the bulk heterojunction layer to the ITO electrode via the PEDOT:PSS layer. In this case, if we simply consider the flat energy band diagram (see Figure 3 inset), even though the detailed band bending after Fermi level alignment should be taken into account, the hole injection from the bulk heterojunction layer (mainly from P3HT) has negative offset energy (-0.3 eV) that is corresponded to no energy barrier for the hole injection. Above the open circuit condition, in contrast, the hole injection direction is inverted so that the hole injection barrier becomes positive (band offset energy = 0.3 eV). However, this offset energy is too small to have influence on the large change in the series resistance. So it is reasonable to consider another major factor that resulted in the large dif-

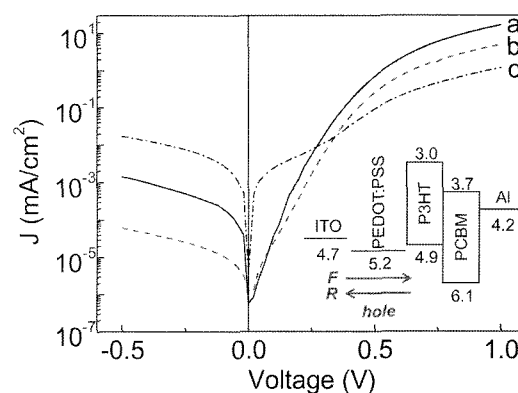


Figure 3. Dark *J-V* characteristics of polymer solar cells with the PEDOT:PSS layer annealed at 25°C (a: black solid line), 120°C (b: red dashed line), and 200°C (c: blue dash-dot line): Inset shows the ideal flat energy band diagram in which 'F' and 'R' denote the direction of hole transport in the PEDOT:PSS layer at forward and reverse bias, respectively.

ference in the J-V curve shape (series resistance) by thermal annealing.

Another noticeable change in the device performance by annealing the PEDOT:PSS layer at 120 °C is the increased open circuit voltage (V_{OC}). Interestingly, further annealing at 200 °C delivered further increase in the open circuit voltage in the presence of much worse series resistance (see the J-V curve shape in Figure 2(c)) [We note that the present devices showed lower V_{OC} than the optimized devices since the active layer was unannealed]. This increased open circuit voltage by thermal annealing could not be attributed to the enhanced photovoltage due to harvested photoelectrons, since the short current density of the device with the PEDOT:PSS layer annealed at 200 °C was rather reduced from that annealed at 120 °C. Hence we suggest the generation of new interfacial layer on top of the PEDOT:PSS layer by thermal annealing, and this layer might be getting thicker if the PEDOT:PSS layer is annealed at higher temperatures. Here, considering the increased open circuit voltage, this newly generated layer should have higher level of highest occupied molecular orbital (HOMO) energy than that of the unannealed PEDOT:PSS surface. Based on the related previous report, we consider that the main part of this new layer would be PSS.¹⁰

In terms of physical shunt resistance, the device with the PEDOT:PSS layer annealed at 120 °C was better than other two devices (see the negative voltage part of the J-V curves in Figure 3). The worse shunt resistance for the device with the PEDOT:PSS layer annealed at 200 °C can be attributed to the possible formation of pin-holes or defects made upon thermal annealing at the high temperature. These defects would affect the series resistance as well.

As summarized in Table I, in spite of the improved shunt resistance (see Figure 3), the fill factor (FF) of the device with the PEDOT:PSS layer annealed at 120 °C was slightly lower than that of the device with the PEDOT:PSS layer annealed at 25 °C. This slightly reduced fill factor might be related to the complex phenomenon combined with the new layer (PSS) formed upon thermal annealing, because the fill factor was much worsened for the device with the PEDOT:PSS layer annealed at 200 °C. Despite the slightly reduced fill factor, the highest power conversion efficiency (PCE) was achieved for the device with the PEDOT:PSS layer annealed at 120 °C owing to the dual increasing effect

Table I. Summary of Polymer Solar Cell Characteristics: T_A Denote the Annealing Temperature of PEDOT:PSS Layer

T_A (°C)	J_{SC} (mA/cm ²)	V_{OC} (mV)	FF (%)	PCE (%)
25	4.32	481	47.8	1.17
120	5.50	560	45.0	1.63
200	4.41	574	33.1	0.99

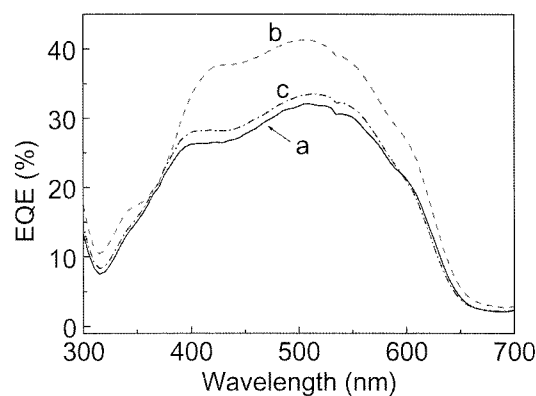


Figure 4. EQE spectra of polymer solar cells with the PEDOT:PSS layer annealed at 25 °C (a: black solid line), 120 °C (b: red dashed line), and 200 °C (c: blue dash-dot line).

of short circuit current density and open circuit voltage.

As shown in Figure 4, the external quantum efficiency spectra exhibit typical shape of P3HT:PCBM (1:1) devices.⁵ The spectral shape is almost identical for the present three devices irrespective of the annealing temperature of the PEDOT:PSS layer. This indicates that no special interaction or reaction was made between the bulk heterojunction layer and the newly formed layer (supposed to be PSS¹⁰) by thermal annealing of PEDOT:PSS layer in the present wavelength range. We note that the order of intensity is also in good agreement with the trend of power conversion efficiency measured under the simulated solar light illumination (AM 1.5).

In summary, we find that the performance of polymer solar cells was influenced by the annealing temperature of thin (20 nm thick) PEDOT:PSS layer. The device with the PEDOT:PSS layer annealed at 120 °C exhibited the highest power conversion efficiency. In particular, the open circuit voltage was increased as the annealing temperature increased, indicating the formation of new layer on top of the annealed PEDOT:PSS layer. However, based on the external quantum efficiency spectra, no evidence was found for the generation of extra excitons by special interaction between this newly formed layer and the bulk heterojunction layer. Finally we suggest that an improved V_{OC} could be achieved if applying a hole-conducting polymer nanolayer.¹¹

Acknowledgements. The authors thank Merck Chemicals Ltd for supplying P3HT materials and financial support from the Korea Science and Engineering Foundation (KOSEF grant (MOST) (No. R01-2007-000-10836-0)).

References

- (1) R. F. Service, *Science*, **309**, 548 (2005).
- (2) Y. Kim, Ph.D Thesis, Imperial College London (2006).

- (3) C. W. Tang, *Appl. Phys. Lett.*, **48**, 183 (1986).
- (4) C. J. Brabec, N. S. Sariciftci, and J. C. Hummelen, *Adv. Funct. Mater.*, **11**, 15 (2001).
- (5) Y. Kim, S. A. Choulis, J. Nelson, D. D. C. Bradley, S. Cook, and J. R. Durrant, *Appl. Phys. Lett.*, **86**, 063502 (2005).
- (6) M. Reyes-Reyes, K. Kim, and D. L. Carroll, *Appl. Phys. Lett.*, **87**, 083506 (2005).
- (7) G. Li, V. Shrotriya, Y. Yao, and Y. Yang, *J. Appl. Phys.*, **98**, 043704 (2005).
- (8) Y. Kim, S. Cook, S. M. Tuladhar, S. A. Choulis, J. Nelson, J. R. Durrant, D. D. C. Bradley, M. Giles, I. McCulloch, C. S. Ha, and M. Ree, *Nature Mater.*, **5**, 197 (2006).
- (9) J. Xue, S. Uchida, B. P. Rand, and S. R. Forrest, *Appl. Phys. Lett.*, **85**, 5757 (2004).
- (10) F. L. Zhang, A. Gadisa, O. Inganas, M. Svensson, and M. R. Andersson, *Appl. Phys. Lett.*, **84**, 3906 (2004).
- (11) J. Keum, C. S. Ha, and Y. Kim, *Macromol. Res.*, **14**, 401 (2006).
- (12) S. H. Jin, D. S. Koo, C. K. Hwang, J. Y. Do, Y. I. Kim, Y. S. Gal, J. W. Lee, and J. T. Hwang, *Macromol. Res.*, **13**, 114 (2005).